

Accelerating Antimicrobial Peptide Discovery with Latent Sequence-Structure Model

Danqing Wang^{1*}, Zeyu Wen², Fei Ye², Lei Li^{1*}, Hao Zhou^{3*}

¹ University of California, Santa Barbara

² ByteDance AI Lab

³ Institute for AI Industry Research, Tsinghua University

danqingwang@ucsb.edu, wenzeyu@bytedance.com, yefei.joyce@bytedance.com,

leili@cs.ucsb.edu, zhouhao@air.tsinghua.edu.cn

Abstract

Antimicrobial peptide (AMP) is a promising therapy in the treatment of broad-spectrum antibiotics and drug-resistant infections. Recently, an increasing number of researchers have been introducing deep generative models to accelerate AMP discovery. However, current studies mainly focus on sequence attributes and ignore structure information, which is important in AMP biological functions. In this paper, we propose a latent sequence-structure model for AMPs (LSSAMP) with multi-scale VQ-VAE to incorporate secondary structures. By sampling in the latent space, LSSAMP can simultaneously generate peptides with ideal sequence attributes and secondary structures. Experimental results show that the peptides generated by LSSAMP have a high probability of AMP, and two of the 21 candidates have been verified to have good antimicrobial activity. Our model will be released to help create high-quality AMP candidates for follow-up biological experiments and accelerate the whole AMP discovery¹.

1 Introduction

In recent years, the development of neural networks for drug discovery has attracted increasing attention. It can facilitate the discovery of potential therapies and reduce the time and cost of drug development (Stokes et al. 2020). Great success has been achieved in applying deep generative models to accelerate the discovery of potential drug-like molecules (Jin et al. 2018; Shi et al. 2019; Schwalbe-Koda and Gómez-Bombarelli 2020; Xie et al. 2020).

Antimicrobial peptides (AMPs) are one of the most promising emerging therapeutic agents to replace antibiotics. They are short proteins which can kill bacteria by destroying the bacterial membrane (Aronica et al. 2021; Cardoso et al. 2020). Compared with the chemical interactions between antibiotics and bacteria that can be avoided by bacterial evolution, this physical mechanism is more difficult to resist.

A typical antimicrobial discovery process usually consists of four steps, as shown in Figure 1. First, a candidate library is built based on the existing AMPs database. These candidates can be created by applying manual heuristic approaches

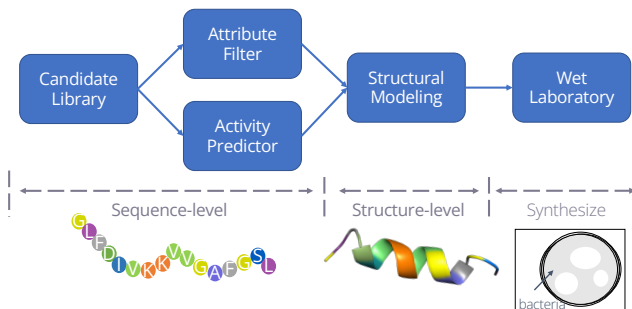


Figure 1: The overview of AMP discovery. The first two steps focus on sequence attributes and the third models the structure. The final step is to verify the antimicrobial activity by inhibiting the growth of bacteria. The grey region is the bacterial suspension and the white one means the bacteria concentration in this region is small.

or training deep generative models. Then, several sequence-based filters are created to screen candidate peptides based on different chemical features, including computational metrics and predictive models trained to estimate ideal properties. After that, to ensure that these sequences can fold into appropriate structures with biological functions, the structure of these sequences will be modelled using peptide structure predictors such as PEPFold 3 (Shen et al. 2014) and molecule dynamics simulations will be performed. Finally, the filtered sequences will be synthesized and tested in the wet laboratory.

Recently, deep generative models have achieved great success in accelerating AMP discovery. They use sequence attributes to control the generation and directly generate peptides with ideal attributes directly (Das et al. 2018, 2021; Van Oort et al. 2021). However, these studies only consider sequence features and ignore the structure-activity relationship. The generated sequences still need to be fed into structure predictors and checked manually, which slows down the discovery process. Besides, the structure also plays an important role in determining biological attributes, which in turn facilitates attribute control (Chen et al. 2019; Torres et al. 2018; Tucker et al. 2018).

In this paper, we incorporate the structure information

*This work is done in ByteDance.

Copyright © 2023, Association for the Advancement of Artificial Intelligence (www.aaai.org). All rights reserved.

¹Code is released in <https://github.com/dqwang122/LSSAMP>.

into the generative model and propose a Latent Sequence-Structure model for AntiMicrobial Peptide (LSSAMP). It maps the sequence features and secondary structures into the same latent space, and samples the peptides with ideal sequence compositions and structures. LSSAMP controls the generation in a more fine-grained manner by assigning a latent variable to each position instead of a continuous variable to control the attributes of the whole sequence. We employ a multi-scale vector quantized-variational autoencoder (VQ-VAE) (van den Oord, Vinyals, and Kavukcuoglu 2017) to capture patterns of different lengths on sequences and structures. During the generation process, LSSAMP samples from the latent space and generates a peptide sequence with its secondary structure. The experimental results via public AMP predictors show that the peptides generated by LSSAMP have a high probability of AMP. We further conduct a comprehensive qualitative analysis, which indicates that our model captures the sequence and structure distribution. We select 21 generated peptides and conduct wet laboratory experiments, and find that 2 of them have high antimicrobial activity against Gram-negative bacteria.

To conclude, our contributions are as follows:

- We propose LSSAMP, a sequence-structure generative model that combines secondary structure information into the generation. It can further accelerate AMP discovery by merging the first three steps together.
- We develop a multi-scale VQ-VAE to control the generation in a fine-grained manner and map patterns in sequences and structures into the same latent space.
- Experimental results of AMP predictors show that LSSAMP generates peptides with high probabilities of AMP. Moreover, 2 of 21 generated peptides show strong antimicrobial activities in wet laboratory experiments.

2 Related work

Antimicrobial Peptide Generation Traditional methods for AMP discovery can be divided into three approaches (Torres and de la Fuente-Nunez 2019): (i) *Pattern recognition algorithms* first builds an antimicrobial sequential pattern database from existing AMPs. Each time a template peptide is chosen to substitute local fragments with those patterns (Loose et al. 2006; Porto et al. 2018). (ii) *Genetic algorithms* use the AMP database to design some antimicrobial activity functions, and optimize ancestral sequences with these functions (Maccari et al. 2013). (iii) *Molecular modeling and molecular dynamics methods* build 3D models of peptides and evaluate their antimicrobial activity by the interaction between peptides and the bacterial membrane (Matyus, Kandt, and Tieleman 2007; Bolinteanu and Kaznessis 2011). Pattern recognition and genetic algorithm bottleneck on representing patterns, and the modeling and dynamics method is computationally expensive and time-consuming.

Deep generative models take a rapid growth in recent years. Dean and Walper (2020) encodes the peptide into the latent space and interpolates across a predictive vector between a known AMP and its scrambled version to generate novel peptides. The PepCVAE (Das et al. 2018) and CLaSS (Das et al. 2021) employ the variational auto-encoder model to

generate sequences. The AMPGAN (Van Oort et al. 2021) uses the generative adversarial network to generate new peptide sequences with a discriminator distinguishing the real AMPs and artificial ones. To our knowledge, this is the first study to incorporate secondary structure information into the generative phase, which is conducive to efficiently generating well-structured sequences with desired properties.

Sequence Generation via VQ-VAE The variational auto-encoders (VAEs) were first proposed by Kingma and Welling (2014) for image generation, and then widely applied to sequence generation tasks such as language modeling (Bowman et al. 2016), paraphrase generation (Gupta et al. 2018), machine translation (Bao et al. 2019) and so on. Instead of mapping the input to a continuous latent space in VAE, the vector quantized-variational autoencoder (VQ-VAE) (van den Oord, Vinyals, and Kavukcuoglu 2017) learns the codebook to obtain a discrete latent representation. It can avoid issues of posterior collapse while has comparable performance with VAEs. Based on it, Razavi, van den Oord, and Vinyals (2019) uses a multi-scale hierarchical organization to capture global and local features for image generation. Bao et al. (2021) learns implicit categorical information of target words with VQ-VAE and models the categorical sequence with conditional random fields in non-autoregressive machine translation. In this paper, we employ the multi-scale vector quantized technique to obtain the discrete representation for each position of the peptide.

3 Method

In this section, we first introduce how existing generative models accelerate this process and their limitations on sequence properties. Thus, we investigate the popular VAE-based models for peptide generation. Based on this, we introduce Latent Sequence-Structure model for AMP (LSSAMP), which uses the multi-scale VQ-VAE to map the sequence and structure distribution into the same latent space and sample peptides with ideal sequence and structures at the same time.

Notations The peptide² is a short protein of amino acids. A peptide with length L can be denoted as $\mathbf{x} = \{x_1, x_2, \dots, x_L\}$. The amino acid x_i in the i -th position belongs to one of the 20 common types and is also called a *residue*. The *secondary structure* is used to describe the local form of the 3D structure of the peptide. Thus, the structure of the peptide can be annotated as $\mathbf{y} = \{y_1, y_2, \dots, y_L\}$, where y_i is the secondary structure label of i -th position, belonging to one of eight types³.

3.1 Antimicrobial Peptide Discovery

Deep generative models have shown promise in accelerating the AMP discovery by combining the sequence-based filters with the generation process and create sequences with user-specified properties as the candidate library directly. However, previous studies only focus on learning sequence features.

²Here, we use the peptide to refer to the oligopeptide (< 20 amino acids) and the polypeptide (< 50 amino acids).

³The three alpha helices are denoted as H, G, and I based on their angles. The two beta sheets are divided into E and T by shape. The others are random coil structures (Kabsch and Sander 1983).

	Uniq	C	H	uH	Combination
VAE (Dean and Walper 2020)	475	18.45% ± 2.92%	2.68% ± 3.28%	-2.78% ± 1.64%	0.29% ± 0.74%
AMP-GAN (Van Oort et al. 2021)	1966	2.79% ± 0.50%	2.16% ± 0.34%	-2.29% ± 0.53%	0.17% ± 0.35%
PepCVAE (Das et al. 2018)	208	3.87% ± 1.58%	-1.93% ± 1.61%	1.01% ± 2.80%	3.93% ± 1.82%
MLPeptide (Capecchi et al. 2021)	2106	-2.48% ± 0.39%	2.01% ± 0.57%	9.24% ± 1.22%	1.12% ± 0.38%

Table 1: The delta ratio of the sequence properties filtered by the secondary structures. **Uniq** is the uniq peptide number in 5000 generated sequences. **C**, **H**, **uH** correspond to charge, hydrophobicity, hydrophobic moment. **Combination** is the percentage of satisfying three ranges at the same time.

They still need to check and filter the structures by external tools after generating sequences, which makes the generation process inefficient. For example, Van Oort et al. (2021) selected 12 cationic and helical peptides among generated peptides, and Capecchi et al. (2021) used the percentage of the predicted α -helix structure fraction to filter peptides after generation.

Besides, there is a close relationship between the structure and activity of peptides. We investigate the effect of secondary structure on sequence properties by filtering the generated sequences based on the proportion of α -helices, which is the most common secondary structure in AMPs. In Table 1, we use three sequence attributes (*charge*, *hydrophobicity*, *hydrophobic moment*) that are crucial for AMP mechanism to evaluate generation performance (Yeaman and Yount 2003; Gidalevitz et al. 2003; Wimley 2010)⁴.

The ratio in Table 1 is the difference in performance before and after the secondary structure filter. We can find that most of the results are improved by limiting alpha-helical structures. The results show that by controlling the structure, the sequence properties can be improved. Thus, incorporating the structure information into generative models can not only accelerate discovery by combining all the steps before the wet laboratory, but also improve the sequence properties and make the generative process more efficient.

3.2 VAE-based Generative Models

Given a sequence \mathbf{x} , the variational auto-encoders assume that it depends on a continuous latent variable \mathbf{z} . Thus the likelihood can be denoted as:

$$p(\mathbf{x}) = \int p(\mathbf{z})p(\mathbf{x}|\mathbf{z})d\mathbf{z}. \quad (1)$$

The controlled sequence generation incorporates the attribute a and models the conditional probability $p(\mathbf{x}|a)$. Based on the dependency between latent variable \mathbf{z} and attribute a , these peptide generative models can be divided into semi-VAEs, such as PepCVAE (Das et al. 2018), and GM-VAEs, such as CLaSS (Das et al. 2021).

Training The vanilla VAE are usually trained in an auto-encoder framework with regularization. The encoder parameterizes an approximate posterior distribution $q_\phi(\mathbf{z}|\mathbf{x})$ and the decoder reconstructs \mathbf{x} based on the latent \mathbf{z} . The models optimizes a evidence lower bound (ELBO):

$$L_r = E_{q_\phi(\mathbf{z}|\mathbf{x})}[\log(p_\theta(\mathbf{x}|\mathbf{z}))] - \text{KL}(q_\phi(\mathbf{z}|\mathbf{x})||p(\mathbf{z})), \quad (2)$$

⁴The definition of these three attributes and detailed experiment descriptions can be found in Appendix.

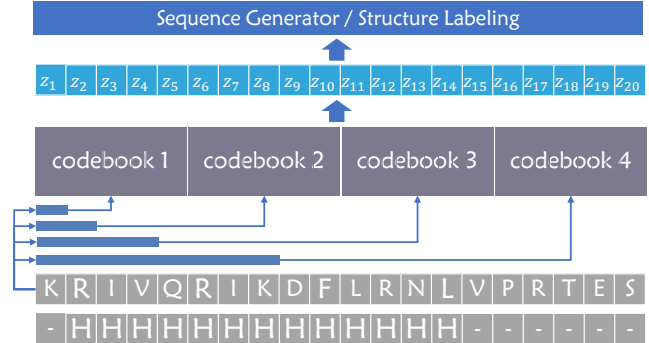


Figure 2: The encoder of LSSAMP. Here, we use $N = 4$ pattern selectors to select local patterns with different scales and use the corresponding codebooks to obtain discrete latent variables z_i for each position. The number of selectors is further discussed in Section 4.4.

where the $E_{q_\phi(\mathbf{z}|\mathbf{x})}[\log(p_\theta(\mathbf{x}|\mathbf{z}))]$ is the reconstruction loss and the KL divergence is the regularization. For conditional generation, the attributes are directly added to the latent variable \mathbf{z} , or trained on the latent space to get an attribute-conditioned posterior distribution $p(\mathbf{z}|a)$. The VAE-based peptide generative models are first trained on unsupervised peptide or protein sequences, and then trained with specific sequences with biological attribute labels.

Sampling A latent variable \mathbf{z} is sampled from the latent space and then fed to the decoder to generate a new sequence. The attributes control the generation with the latent \mathbf{z} .

3.3 Latent Sequence-Structure Model

To address these challenges, we combine the secondary structure with sequence attributes to further accelerate the discovery and build a more effective candidate library. Different from previous work, we assign a latent variable z_i for each x_i instead of a continuous \mathbf{z} for the whole sequence. This gives our model a more fine-grained control on each position. Since it is computationally intractable to sum continuous latent variables over the sequence, we use VQ-VAE (van den Oord, Vinyals, and Kavukcuoglu 2017) to lookup the discrete embedding vector $\mathbf{z}_q = \{z_q(x_1), \dots, z_q(x_L)\}$ for each position by vector quantization.

Specifically, the encoder output $z_i = z_e(x_i) \in \mathbb{R}^d$ will be replaced by the codebook entry $z_q(x_i) \in \mathbb{R}^d$ via a nearest

neighbors lookup from the codebook $\mathbf{B} \in \mathbb{R}^{K \times d}$:

$$z_q(x_i) = e_k, \text{ and } k = \operatorname{argmin}_{j \in \{1, \dots, K\}} \|z_e(x_i) - e_j\|_2. \quad (3)$$

Here, K is the slot number of the codebook and d is the dimension of the codebook entry e . Then, the generator will take $z_q(x_i)$ as its input and reconstruct x_i . The training objective L_r is defined as:

$$L_r = \sum_{i=1}^L \log p(x_i | z_q(x_i)) + \|\operatorname{sg}[z_e(x_i)] - z_q(x_i)\|_2^2 + \beta \|z_e(x_i) - \operatorname{sg}[z_q(x_i)]\|_2^2. \quad (4)$$

Here, $\operatorname{sg}(\cdot)$ is the stop gradient operator, which becomes 0 at the backward pass. β is the commit coefficient to control the codebook loss. The $\sum_{i=1}^L \log p(x_i | z_q(x_i))$ is the discrete reconstruction loss and the rest components perform as the KL divergence regularization, like the second term in Eqn. 2.

We add a 8-category labeling task on the latent space to incorporate the secondary structure information. $z_{q'}(x_i)$ is fed to a separate classifier for the structure prediction. The training objective L_s is similar to Eqn. 4 except that the first term is a supervised version $\sum_{i=1}^L \log p(y_i | z_{q'}(x_i))$. The sequence and structure codebook are not necessary the same, thus we use $z_{q'}(x_i)$ to indicate the structure latent variable.

However, the structure motifs are often longer than chain patterns. Therefore, we establish multiple codebooks to capture features of different scales.

Multi-scale VQ-VAE The structure motifs are often longer than sequence patterns. For example, a valid α -helix contains at least 4 residues and may be longer than 12. However, sequence patterns with specific biological functions are much shorter, usually between 1 and 8 residues. In order to capture these features and map them into the same latent space, we first apply N multi-scale pattern selectors F_n . Then, we establish multiple codebooks and use Eqn. 3 to look up the nearest codebook embedding $z_{q_n}(x_i)$. We share the codebooks between sequence reconstruction and secondary structure prediction to capture common features and relationships between the residue and its structure. The concatenated multi-scale codebook embedding is fed to the sequence generator:

$$z_q(x_i) = \parallel_{n \in N} z_{q_n}(x_i), \quad (5)$$

Based on Eqn. 4, the reconstruction training objective for multi-scale VQ-VAE can be adapted as the sum of loss on multiple codebooks.

Thus, the total training loss is composed of the reconstruction loss and the labeling loss, which can be denoted as:

$$L = L_r + \gamma L_s, \quad (6)$$

where the γ is the weight of the structure prediction task.

Training As VAE-based generative models, we first train LSSAMP in a unsupervised manner with protein sequences via L_r . Then, we incorporate the structure information by jointly training L_r and L_s on a smaller protein dataset

Algorithm 1: Training and Sampling phase of LSSAMP

Require: A protein dataset D_r , a peptide dataset with secondary structure D_s , and the AMP dataset D_{amp} . The model M_θ with N codebooks. A set of N prior models M_{prior_n} .

- 1: Train on D_r and update M_θ via Eqn. 4.
 - 2: Train on D_s and update the M_θ via Eqn. 6.
 - 3: Finetune M_θ on D_{amp} via Eqn. 6.
 - 4: **for** each codebook $n = 1, 2, \dots, N$ **do**
 - 5: Create an empty dataset C_n .
 - 6: **for** $x_i \in D_{amp}$ **do**
 - 7: Save the n -th codebook index of x_i via Eqn. 3 to C_n
 - 8: **end for**
 - 9: Train an auto-regressive language model M_{prior_n} on C_n .
 - 10: **end for**
-

with secondary structure annotation. Finally, we finetune our model on the AMP dataset to capture the specific AMP characteristics. The whole training process is described in Algorithm 1.

Following Kaiser et al. (2018), we use Exponential Moving Average (EMA) to update the embedding vectors in the codebooks. Specifically, we keep a count c_k measuring the number of times that the embedding vector e_k is chosen as the nearest neighbor of $z_e(x_i)$ via Eqn. 3. Thus, the counts are updated with a sort of momentum: $c_k \leftarrow \lambda c_k + (1 - \lambda) \sum_i \mathbb{I}[z_q(x_i) = e_k]$, with the embedding e_k being updated as: $e_k \leftarrow \lambda e_k + (1 - \lambda) \sum_i \frac{\mathbb{I}[z_q(x_i) = e_k] z_e(x_i)}{c_k}$. Here, λ is the decay parameter.

Prior Model The prior distribution over the codebook is a categorical distribution and can be made auto-regressive by the extra prior model. In order to model the dependency between $z_{1:L}$, we train Transformer-based language models on the embedding entries. We extract the index sequences generated by Eqn. 3 for each codebook n and then train M_{prior_n} on them.

Sampling We sample several index sequences from the prior models for each codebook n , and then lookup the codebook to get the embedding vector z_{q_n} . Finally, z_{q_n} is fed to the generator and classifier to generate the sequence with its secondary structure. We also try to control the secondary structure by existing AMP structure patterns to further improve the generation quality.

4 Experiment

4.1 Experiment Setup

Dataset The Universal Protein Resource (UniProt)⁵ is a comprehensive protein dataset. We download reviewed protein sequences (550k) with the limitation of 100 in length as D_r (57k examples). Then we use a community reimplementation of AlphaFold (AlQuraishi 2019), which is called ProSPR⁶ (Billings et al. 2019) to predict the secondary structure for D_r . After filtering some low-quality examples, we obtain D_s with 46k examples, including both sequence and secondary structure information. For antimicrobial peptide dataset, we download from Antimicrobial Peptide Database

⁵<https://www.uniprot.org/>

⁶<https://github.com/dellacortelab/prospr/tree/prospr1>

	SVM	RF	DA	Scanner	AMPMIC	IAMPE	amPEP	Average
APD	87.78%	91.24%	86.24%	94.66%	98.42%	97.83%	91.50%	92.52%
Decoy	17.43%	13.71%	16.04%	0.25%	18.07%	23.53%	52.92%	20.28%
Random $p = 0.1$	86.06%	86.12%	84.01%	93.23%	79.14%	95.60%	91.74%	87.99%
Random $p = 0.2$	76.66%	76.64%	74.83%	86.95%	68.57%	91.14%	87.89%	80.38%
VAE (Dean and Walper 2020)	24.90%	15.30%	13.83%	15.12%	15.25%	40.31%	24.30%	21.29%
AMP-GAN (Van Oort et al. 2021)	78.62%	87.29%	83.82%	82.17%	89.58%	93.88%	80.52%	85.13%
PepCVAE (Das et al. 2018)	82.84%	85.96%	93.33%	85.44%	98.44%	98.14%	80.77%	89.27%
MLPeptide (Capecchi et al. 2021)	90.43%	92.55%	93.08%	93.72%	96.34%	97.05%	91.37%	93.51%
LSSAMP	92.03%	92.60%	93.45%	91.52%	95.84%	96.64%	93.23%	93.62%
LSSAMP w/o cond	78.98%	80.24%	80.01%	86.73%	83.81%	93.80%	85.32%	84.13%

Table 2: The percentage of generated sequences being predicted as AMP. The classifiers are described in Section 4.2. The first part is the prediction results on AMP and non-AMP dataset as the reference. The bold ones are the best model results.

(APD3)⁷ (Wang, Li, and Wang 2016) and filter repeated ones to get 3222 AMPs as D_{amp} . We randomly extract 3,000 examples as validation and 3,000 as test on D_r and D_s . For D_{amp} , the size of validation and test is both 100. Following Veltri, Kamath, and Shehu (2018), we create a decoy set of negative examples without antimicrobial activities for comparison. It removes peptide sequences with antimicrobial activity from Uniprot, and sequences with length < 10 or > 40 , resulting in 2021 non-AMP sequences.

Baseline Traditional methods usually randomly replace several residues on existing AMPs and conduct biological experiments on them. Thus, we use **Random** baseline to represent the method of replacing each residue with probability p . Following Dean and Walper (2020), we use **VAE** to embed the peptides into the latent space and sample latent variable z from the standard Gaussian distribution $p \sim N(0, 1)$. For a fair comparison, we use the same Transformer architecture as our model **LSSAMP** and train on the Uniprot D_r and APD dataset D_{amp} . **AMP-GAN** is proposed by Van Oort et al. (2021), which uses a BiCGAN architecture with convolution layers. It consists of three parts: the generator, discriminator, and encoder. The generator and discriminator share the same encoder. It is trained on 49k false negative sequences from UniProt and 7k positive AMP sequences. **PepCVAE** is a semi-VAE generative model that concatenates the attribute features to the latent variable for conditional generation (Das et al. 2018). Since the authors did not release their code, we use the model architecture from Hu et al. (2017) and modify the reproduced code⁸ for AMPs, as described in their paper. The original paper uses 93k sequences from UniProt and 7960/6948 positive/negative AMPs for training. For comparison, we use UniProt dataset D_r and ADP dataset D_{amp} to train it. **MLPeptide** (Capecchi et al. 2021) is RNN-based generator. It is first trained on 3580 AMPs and then transferred to specific bacteria. **LSSAMP** is implemented as described in Section 3.3. The detailed hyperparameters are discussed in Appendix.

Implementation details There are three main modules

⁷<https://aps.unmc.edu/>

⁸<https://github.com/wiseodd/controlled-text-generation>

	Uniqueness \uparrow	Diversity \uparrow	Novelty \uparrow
Random $p = 0.1$	0.995 \pm 0.000	0.871 \pm 0.021	0.078 \pm 0.001
Random $p = 0.2$	0.999 \pm 0.000	0.971 \pm 0.022	0.160 \pm 0.001
VAE	0.986 \pm 0.001	1.011 \pm 0.038	0.584 \pm 0.002
AMP-GAN	0.995 \pm 0.001	0.907 \pm 0.023	0.565 \pm 0.007
PepCVAE	0.265 \pm 0.006	0.367 \pm 0.007	0.423 \pm 0.005
MLPeptide	0.900 \pm 0.003	0.850 \pm 0.016	0.416 \pm 0.010
LSSAMP	0.981 \pm 0.001	0.878 \pm 0.018	0.503 \pm 0.005
LSSAMP w/o cond	0.976 \pm 0.002	0.901 \pm 0.013	0.515 \pm 0.008

Table 3: The novelty of the sampling. \uparrow means higher is better. The detailed descriptions are in Section 4.2.

for **LSSAMP**. The encoder and decoder are based on 2-layer Transformer (Vaswani et al. 2017) with $d_{model} = 128$, $head = 8$. The size of FFN projection is $d_{ffn} = 512$ and all dropout rate are 0.1. For the classifier, we use the same CNN block as Billings et al. (2019) with 32 input channels and a dilation scale of [1, 2, 4, 8, 10]. For multi-scale codebooks, we first apply CNN as $F^{(n)}$ to extract features. We set $n = 4$ and kernel width ranging in [1, 2, 4, 8]. The features will be padded to the same length as the input sequence. Then, we use 4 codebooks with $K = 8$ and $d = 128$. The reconstruction and prediction share the same codebooks, which means $N_r = N_s = 4$. The commit coefficient is set to $\beta = 0.05$.

We use PyTorch to implement our model and train it on a single Tesla-V100-32GB. We optimize the parameter with Adam Optimizer (Kingma and Ba 2015). During pre-training for sequence construction on D_r , we set the maximum token in a batch bz as 30,000, learning rate lr as 0.01 with 8,000 warm-up steps, and decoy weight for EMA as $\lambda = 0.8$. For secondary structure prediction on D_s , the max length is limited to 32, $bz = 10,000$, $lr = 0.003$, $\lambda = 0.95$, and the prediction loss coefficient $\gamma = 1$. Finally, we transfer to D_{amp} with the same hyperparameters except the $lr = 0.001$.

4.2 Evaluation Metric

Following previous work (Das et al. 2020; Van Oort et al. 2021), we use open-source AMP prediction tools to estimate the AMP probability of the generated sequence. Since these

No	Sequence	Activity (ug/mL) ↓			Sequence identity ↓	Hemolysis/Toxicity ↓
		A. Baumannii	P. aeruginose	E. coli		
P1	GAFGNFLKNVAKKAGIYLLSIAQCCKLFGTP	16-32	/	32-64	83.30%	Low
P2	FIGFLFKLAKKIIPSLFQTKTE	8	32	/	75.00%	Low

Table 4: Wet laboratory experiment results. The activity is measured by MIC and ↓ means the lower the better. ‘Sequence identity’ measures the similarity with existing AMPs and ‘Hemolysis/Toxicity’ measures the damage to other cells.

open-source AMP predictors are trained and report results in different AMP datasets, we use them to predict sequences in APD and decoy datasets as a reference of their performance. We also evaluate the generative diversity of these models.

AMP Classifiers Thomas et al. (2010) trained on the AMP database of 3782 sequences with random forest (RF), discriminant analysis (DA), support vector machines (SVM)⁹, and artificial neural network (ANN)¹⁰ respectively. AMP Scanner v2¹¹ (Veltri, Kamath, and Shehu 2018), short as **Scanner**, is a CNN-&LSTM-based deep neural network trained on 1778 AMPs picked from APD. **AMPMIC**¹² (Witten and Witten 2019) trained a CNN-based regression model on 6760 unique sequences and 51345 MIC measurement to predict MIC values. **IAMPE**¹³ (Kavousi et al. 2020) is a model based on Xtreme Gradient Boosting. It achieves the highest correct prediction rate on a set of ten more recent AMPs (Aronica et al. 2021). **ampPEP**¹⁴ (Lawrence et al. 2021) is a random forest based model which is trained on 3268 AMP sequences. It has the best performance across multiple datasets (Aronica et al. 2021).

Novelty To measure the novelty of the generated peptides, we define three evaluation metrics: Uniqueness, Diversity, and Similarity. **Uniqueness** is the percentage of unique peptides in the generation phase. **Diversity** measures the similarity among the generated peptides. We calculate the Levenshtein distance (Levenshtein et al. 1966) between every two sequences and normalize it by the sequence length. Then we average the normalized distance to get the mean as its diversity. The higher the diversity, the more dissimilar the generated peptides are. **Novelty** is the difference between the generated peptides and the training AMP set. For each generated sequence, we search the training set for a peptide which has the smallest Levenshtein distance from it and normalize the distance according to its length. We calculate the average length as the Novelty.

4.3 Experimental Results

We generate 5000 sequences for each baseline. During the generation process, we add some structural restrictions on positions based on the antimicrobial mechanism. Specifically, we reject peptides with more than 30% coil structure (‘-’), which can hardly fold in the solution environment and insert

⁹<http://www.camp3.bicnirrh.res.in/prediction.php>

¹⁰We drop the ANN model because its accuracy on APD is low (82.83%).

¹¹<https://www.dveltri.com/ascan/v2/ascan.html>

¹²<https://github.com/zswitten/Antimicrobial-Peptides>

¹³<http://cbb1.ut.ac.ir/AMPClassifier/Index>

¹⁴<https://github.com/lawrence3/amPEPpy>

	PPL ↓	Loss ↓	AA Acc. ↑	SS Acc. ↑
LSSAMP	3.12	1.14	99.93	86.76
w/o D_r	11.56	2.45	66.06	82.78
w/o D_s	3.83	1.34	99.58	85.87
w/o subbook	3.49	1.25	99.86	86.61

Table 5: Ablation Study on validation set of D_{amp} . ‘w/o’ indicates that we remove the module from LSSAMP.

Codebook	PPL ↓	Loss ↓	AA Acc. ↑	SS Acc. ↑
[1]	19.04 ± 2.84	2.94 ± 0.14	65.49 ± 3.49	83.41 ± 2.34
[1, 2]	3.84 ± 0.09	1.35 ± 0.02	99.40 ± 0.45	85.39 ± 0.26
[1, 2, 4]	3.32 ± 0.03	1.20 ± 0.01	100.00 ± 0.00	85.95 ± 0.42
[1, 2, 4, 8]	3.24 ± 0.16	1.17 ± 0.05	99.79 ± 0.20	87.20 ± 0.62

Table 6: The influence of the number of codebooks. ‘[1,2,4,8]’ indicates that we use 4 codebooks with window sizes of 1,2,4,8. The meanings of symbols are the same as Table 5.

into the bacterial membrane in silico screening. Besides, we limit the minimum length of a continuous helix (‘H’) to 4 according to physical rules. We name our model with structural control as **LSSAMP** and the model without extra conditions as **LSSAMP w/o cond**.

AMP Prediction The results of prediction tools are shown in Table 2. LSSAMP performs best in four of seven and have a highest average score across all classifiers, indicating its advantage over baselines. PepCVAE performs best on the AMP-MIC and IAMPE predictors, however, it performs poorly on the other predictors and gets a low average score. MLPeptide performs relatively evenly across predictors, outperforming other models on only Scanner and slightly underperforming our model on the average score. The comparison of LSSAMP and LSSAMP w/o cond indicates that add fine-grained control on the secondary structure can further improve the generation performance.

Novelty From Table 3, we can see that VAE has the highest diversity and novelty. However, from Table 2, we can find that the peptides generated by VAE do not have a high probability of AMP. It means that the vanilla VAE trained on AMP datasets without attribute control can hardly capture the antimicrobial features. It randomly samples in the latent space. At the same time, LSSAMP has a significant advantage over the above strong baseline PepCVAE and MLPeptide. It means that our model can generate promising AMPs with relatively high novelty. Besides, the limitation of secondary structure will lead to a decline in diversity. However, it does

ID	Sequence	Secondary Structure	C	H	uH
1	FLPLVRVWAKLI	-HHHHHHHHHHH	2.0	0.471	0.723
2	FLSTVPYVAFKVVPTLFCPIAKTC	-HHHHHHHHHHHHHHHHHHHHHT-	2.0	0.446	1.812
3	FFGVLARGIKSVVKHVMGLLMG	-HHHHHHHHHHHHHHHHHHHH-	3.0	0.420	0.549
4	GVLPAFKQYLPGIMKIIVKF	-HHHHHHHHHHHHHHHHHH-	3.0	0.419	0.523
5	VFTLLGAIHHHLGNFVKRFSHVF	-HHHHHHHHHHHHHHHHHHHH-	2.0	0.416	0.514
6	FVPLGIKAAVGIGYTIFCKISKACYQ	-HHHHHHHHHHHHHHHHHHHT-	3.0	0.394	1.815
7	ALWCQMLTGIGKLAGKA	-HHHHHHHHHHHHHHHHH	2.0	0.344	0.506
8	LLTRIIVGSAVTSLIKKS	-HHHHHHHHHHHHHHHHH-	3.0	0.334	0.531
9	FLSVIKGVWAASLPKQFCAVTAKC	-HHHHHHHHHHHHHHHHHHHT-	3.0	0.334	0.660
10	FLNPIIKIATQILVTAIKCFLKKC	-HHHHHHHHHHHHHHHHHHHT-	4.0	0.334	1.940

Table 7: Ten generated peptides and their physical properties and predicted structures. ‘H’ is the α -helix, ‘T’ is the Turn and ‘-’ is the coil.

not result in more redundant peptides because the uniqueness does not decrease. It indicates that the restrictions make the model capture similar local patterns, but not generate the exact same sequence.

Wet Laboratory Experiment We further synthesize and experimentally characterize peptides designed with LSSAMP. We select 21 peptides and test their antimicrobial activities against three panels of Gram-negative bacteria (*A. Baumannii*, *P. aeruginosa*, *E. coli*), which costs about 30 days. We use minimal inhibitory concentration (MIC) to evaluate the activity. The details of wet laboratory experiments are described in Appendix. As shown in Table 4, two peptides are both found to be effective against *A. Baumannii*. **P2** against *P. aeruginosa* and **P1** against for *E.coli* also show activity. Besides, these two newly discovered AMPs differ from existing AMPs and have a low toxicity, which means they are promising new therapeutic agents. The wet-lab experiment results demonstrate LSSAMP can effectively find AMP candidates and reduce the time cost.

Ablation Study We conduct the ablation study for our LSSAMP and show the results in Table 5. **PPL** is the perplexity of generated sequences that can measure fluency. **Loss** is the model loss on the validation set. **AA Acc.** is the reconstruction accuracy of residue and **SS Acc.** is the prediction accuracy of the secondary structure. We can find that without the first training phase on D_r , the model can hardly generate valid sequences. The second phase to train the model on the large-scale secondary structure dataset D_s will affect the prediction performance on the target AMP dataset. If we remove multiple sub-codebooks and use a single large codebook with the same size, the performance will decline.

4.4 Analysis

Codebook Number We explore the effect of different numbers of codebooks on generation performance. From Table 6, we find that a single small codebook can hardly learn enough information to reconstruct the sequence. The PPL, Loss, and SS Acc. become better with the increase of codebook entries. However, the reconstruction accuracy achieves the best performance when the codebook is 3. This may be due to the relatively short local pattern of sequences, making the window of 8 too long for it.

Case Study We show 10 peptides generated by LSSAMP

in Table 7. We further build 3D models of 4 generated sequences by PEPFold 3 (Shen et al. 2014) and draw the picture by PyMOL (Schrödinger, LLC 2015) in Figure 3. We can find that all these peptides have several helical structures, which make them more likely to have the antimicrobial ability. At the same time, although the model predicts a long continuous helical structure for ID = 2 and ID = 3, in fact, they have a small coil structure between the two helical structures. It indicates that our model tends to predict a long continuous secondary structure instead of several discontinuous small fragments.

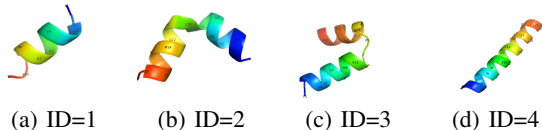


Figure 3: 3D structures for sequence *FLPLVRVWAKLI*, *GVLPAFKQYLPGIMKIIVKF*, *FLSVIKGVWAASLPKQFCAVTAKC*, *FLNPIIKIATQILVTAIKCFLKKC*.

5 Conclusion

In this paper, we propose LSSAMP that uses multi-scale VQ-VAE for fine-grained control of each position. It maps sequential and structural features into the same latent space, and by sampling the overlapping distribution, it can generate peptides with ideal sequence attributes and secondary structures. LSSAMP shows good performance on AMP predictors and designs two peptides with high activity against Gram-negative bacteria. This indicates that our generative model can effectively create an AMP library with high-quality candidates for follow-up biological experiments, which can accelerate the AMP discovery.

Acknowledgement

We thank Wuxi AppTec for conducting the wet laboratory experiments. The work is supported by ByteDance AI Lab.

References

- AlQuraishi, M. 2019. AlphaFold at CASP13. *Bioinformatics*, 35(22): 4862–4865.
- Aronica, P. G.; Reid, L. M.; Desai, N.; Li, J.; Fox, S. J.; Yadahalli, S.; Essex, J. W.; and Verma, C. S. 2021. Computational Methods and Tools in Antimicrobial Peptide Research. *Journal of Chemical Information and Modeling*, 61(7): 3172–3196.
- Bao, Y.; Huang, S.; Xiao, T.; Wang, D.; Dai, X.; and Chen, J. 2021. Non-Autoregressive Translation by Learning Target Categorical Codes. In *Proc. of NAACL-HLT*, 5749–5759.
- Bao, Y.; Zhou, H.; Huang, S.; Li, L.; Mou, L.; Vechtomova, O.; Dai, X.; and Chen, J. 2019. Generating Sentences from Disentangled Syntactic and Semantic Spaces. In *Proc. of ACL*.
- Billings, W. M.; Hedelius, B.; Millecam, T.; Wingate, D.; and Della Corte, D. 2019. ProSPR: democratized implementation of alphafold protein distance prediction network. *bioRxiv*, 830273.
- Bolinteanu, D. S.; and Kaznessis, Y. N. 2011. Computational studies of protegrin antimicrobial peptides: a review. *Peptides*, 32(1): 188–201.
- Boman, H. 2003. Antibacterial peptides: basic facts and emerging concepts. *Journal of internal medicine*, 254(3): 197–215.
- Bowman, S. R.; Vilnis, L.; Vinyals, O.; Dai, A. M.; Jozefowicz, R.; and Bengio, S. 2016. Generating sentences from a continuous space. In *20th SIGNLL Conference on Computational Natural Language Learning, CoNLL 2016*, 10–21. Association for Computational Linguistics (ACL).
- Capecchi, A.; Cai, X.; Personne, H.; Kohler, T.; van Delden, C.; and Reymond, J.-L. 2021. Machine Learning Designs Non-Hemolytic Antimicrobial Peptides. *Chemical Science*.
- Cardoso, M. H.; Orozco, R. Q.; Rezende, S. B.; Rodrigues, G.; Oshiro, K. G.; Cândido, E. S.; and Franco, O. L. 2020. Computer-aided design of antimicrobial peptides: are we generating effective drug candidates? *Frontiers in microbiology*, 10: 3097.
- Chen, C. H.; Starr, C. G.; Troendle, E.; Wiedman, G.; Wimley, W. C.; Ulmschneider, J. P.; and Ulmschneider, M. B. 2019. Simulation-guided rational de novo design of a small pore-forming antimicrobial peptide. *Journal of the American Chemical Society*, 141(12): 4839–4848.
- Das, P.; Sercu, T.; Wadhawan, K.; Padhi, I.; Gehrmann, S.; Cipcigan, F.; Chenthamarakshan, V.; Strobel, H.; Dos Santos, C.; Chen, P.-Y.; et al. 2021. Accelerated antimicrobial discovery via deep generative models and molecular dynamics simulations. *Nature Biomedical Engineering*, 5(6): 613–623.
- Das, P.; Sercu, T.; Wadhawan, K.; Padhi, I.; Gehrmann, S.; Cipcigan, F.; Chenthamarakshan, V.; Strobel, H.; Santos, C. d.; Chen, P.-Y.; et al. 2020. Accelerating Antimicrobial Discovery with Controllable Deep Generative Models and Molecular Dynamics. *arXiv preprint arXiv:2005.11248*.
- Das, P.; Wadhawan, K.; Chang, O.; Sercu, T.; Santos, C. D.; Riemer, M.; Chenthamarakshan, V.; Padhi, I.; and Mojsilovic, A. 2018. Pepcvae: Semi-supervised targeted design of antimicrobial peptide sequences. *arXiv preprint arXiv:1810.07743*.
- Dean, S. N.; and Walper, S. A. 2020. Variational autoencoder for generation of antimicrobial peptides. *ACS omega*, 5(33): 20746–20754.
- Eisenberg, D.; Weiss, R. M.; and Terwilliger, T. C. 1984. The hydrophobic moment detects periodicity in protein hydrophobicity. *Proceedings of the National Academy of Sciences*, 81(1): 140–144.
- Gidalevitz, D.; Ishitsuka, Y.; Muresan, A. S.; Kononov, O.; Waring, A. J.; Lehrer, R. I.; and Lee, K. Y. C. 2003. Interaction of antimicrobial peptide protegrin with biomembranes. *Proceedings of the National Academy of Sciences*, 100(11): 6302–6307.
- Gupta, A.; Agarwal, A.; Singh, P.; and Rai, P. 2018. A Deep Generative Framework for Paraphrase Generation. In McIlraith, S. A.; and Weinberger, K. Q., eds., *Proc. of AAAI*, 5149–5156.
- Hancock, R. E.; and Rozek, A. 2002. Role of membranes in the activities of antimicrobial cationic peptides. *FEMS microbiology letters*, 206(2): 143–149.
- Hu, Z.; Yang, Z.; Liang, X.; Salakhutdinov, R.; and Xing, E. P. 2017. Toward controlled generation of text. In *International Conference on Machine Learning*, 1587–1596. PMLR.
- Jin, W.; Yang, K.; Barzilay, R.; and Jaakkola, T. 2018. Learning Multimodal Graph-to-Graph Translation for Molecule Optimization. In *International Conference on Learning Representations*.
- Kabsch, W.; and Sander, C. 1983. Dictionary of protein secondary structure: pattern recognition of hydrogen-bonded and geometrical features. *Biopolymers: Original Research on Biomolecules*, 22(12): 2577–2637.
- Kaiser, L.; Bengio, S.; Roy, A.; Vaswani, A.; Parmar, N.; Uszkoreit, J.; and Shazeer, N. 2018. Fast decoding in sequence models using discrete latent variables. In *International Conference on Machine Learning*, 2390–2399. PMLR.
- Kavousi, K.; Bagheri, M.; Behrouzi, S.; Vafadar, S.; Atanaki, F. F.; Lotfabadi, B. T.; Ariaeenejad, S.; Shockravi, A.; and Moosavi-Movahedi, A. A. 2020. IAMPE: NMR-assisted computational prediction of antimicrobial peptides. *Journal of Chemical Information and Modeling*, 60(10): 4691–4701.
- Kingma, D. P.; and Ba, J. 2015. Adam: A Method for Stochastic Optimization. In Bengio, Y.; and LeCun, Y., eds., *Proc. of ICLR*.
- Kingma, D. P.; and Welling, M. 2014. Auto-Encoding Variational Bayes.
- Lawrence, T. J.; Carper, D. L.; Spangler, M. K.; Carrell, A. A.; Rush, T. A.; Minter, S. J.; Weston, D. J.; and Labbé, J. L. 2021. amPEPpy 1.0: a portable and accurate antimicrobial peptide prediction tool. *Bioinformatics*, 37(14): 2058–2060.
- Levenshtein, V. I.; et al. 1966. Binary codes capable of correcting deletions, insertions, and reversals. In *Soviet physics doklady*, volume 10, 707–710. Soviet Union.
- Loose, C.; Jensen, K.; Rigoutsos, I.; and Stephanopoulos, G. 2006. A linguistic model for the rational design of antimicrobial peptides. *Nature*, 443(7113): 867–869.
- Maccari, G.; Di Luca, M.; Nifosí, R.; Cardarelli, F.; Signore, G.; Boccardi, C.; and Bifone, A. 2013. Antimicrobial

- peptides design by evolutionary multiobjective optimization. *PLoS computational biology*, 9(9): e1003212.
- Matyus, E.; Kandt, C.; and Tieleman, D. P. 2007. Computer simulation of antimicrobial peptides. *Current medicinal chemistry*, 14(26): 2789–2798.
- Porto, W. F.; Fensterseifer, I. C.; Ribeiro, S. M.; and Franco, O. L. 2018. Joker: An algorithm to insert patterns into sequences for designing antimicrobial peptides. *Biochimica et Biophysica Acta (BBA)-General Subjects*, 1862(9): 2043–2052.
- Razavi, A.; van den Oord, A.; and Vinyals, O. 2019. Generating diverse high-fidelity images with vq-vae-2. In *Advances in neural information processing systems*, 14866–14876.
- Schrödinger, LLC. 2015. The PyMOL Molecular Graphics System, Version 1.8.
- Schwalbe-Koda, D.; and Gómez-Bombarelli, R. 2020. Generative models for automatic chemical design. In *Machine Learning Meets Quantum Physics*, 445–467. Springer.
- Shen, Y.; Maupetit, J.; Derreumaux, P.; and Tuffery, P. 2014. Improved PEP-FOLD approach for peptide and miniprotein structure prediction. *Journal of chemical theory and computation*, 10(10): 4745–4758.
- Shi, C.; Xu, M.; Zhu, Z.; Zhang, W.; Zhang, M.; and Tang, J. 2019. GraphAF: a Flow-based Autoregressive Model for Molecular Graph Generation. In *International Conference on Learning Representations*.
- Stokes, J. M.; Yang, K.; Swanson, K.; Jin, W.; Cubillos-Ruiz, A.; Donghia, N. M.; MacNair, C. R.; French, S.; Carfrae, L. A.; Bloom-Ackermann, Z.; et al. 2020. A deep learning approach to antibiotic discovery. *Cell*, 180(4): 688–702.
- Thomas, S.; Karnik, S.; Barai, R. S.; Jayaraman, V. K.; and Idicula-Thomas, S. 2010. CAMP: a useful resource for research on antimicrobial peptides. *Nucleic acids research*, 38(suppl_1): D774–D780.
- Torres, M. D.; Pedron, C. N.; Higashikuni, Y.; Kramer, R. M.; Cardoso, M. H.; Oshiro, K. G.; Franco, O. L.; Silva Junior, P. I.; Silva, F. D.; Oliveira Junior, V. X.; et al. 2018. Structure-function-guided exploration of the antimicrobial peptide polybia-CP identifies activity determinants and generates synthetic therapeutic candidates. *Communications biology*, 1(1): 1–16.
- Torres, M. D. T.; and de la Fuente-Nunez, C. 2019. Toward computer-made artificial antibiotics. *Current opinion in microbiology*, 51: 30–38.
- Tucker, A. T.; Leonard, S. P.; DuBois, C. D.; Knauf, G. A.; Cunningham, A. L.; Wilke, C. O.; Trent, M. S.; and Davies, B. W. 2018. Discovery of next-generation antimicrobials through bacterial self-screening of surface-displayed peptide libraries. *Cell*, 172(3): 618–628.
- van den Oord, A.; Vinyals, O.; and Kavukcuoglu, K. 2017. Neural discrete representation learning. In *Proceedings of the 31st International Conference on Neural Information Processing Systems*, 6309–6318.
- Van Oort, C. M.; Ferrell, J. B.; Remington, J. M.; Wshah, S.; and Li, J. 2021. AMPGAN v2: Machine Learning-Guided Design of Antimicrobial Peptides. *Journal of Chemical Information and Modeling*.
- Vaswani, A.; Shazeer, N.; Parmar, N.; Uszkoreit, J.; Jones, L.; Gomez, A. N.; Kaiser, L.; and Polosukhin, I. 2017. Attention is All you Need. In Guyon, I.; von Luxburg, U.; Bengio, S.; Wallach, H. M.; Fergus, R.; Vishwanathan, S. V. N.; and Garnett, R., eds., *Proc. of NeurIPS*, 5998–6008.
- Veltri, D.; Kamath, U.; and Shehu, A. 2018. Deep learning improves antimicrobial peptide recognition. *Bioinformatics*, 34(16): 2740–2747.
- Wang, G.; Li, X.; and Wang, Z. 2016. APD3: the antimicrobial peptide database as a tool for research and education. *Nucleic acids research*, 44(D1): D1087–D1093.
- Wimley, W. C. 2010. Describing the mechanism of antimicrobial peptide action with the interfacial activity model. *ACS chemical biology*, 5(10): 905–917.
- Witten, J.; and Witten, Z. 2019. Deep learning regression model for antimicrobial peptide design. *BioRxiv*, 692681.
- Xie, Y.; Shi, C.; Zhou, H.; Yang, Y.; Zhang, W.; Yu, Y.; and Li, L. 2020. MARS: Markov Molecular Sampling for Multi-objective Drug Discovery. In *International Conference on Learning Representations*.
- Yeaman, M. R.; and Yount, N. Y. 2003. Mechanisms of antimicrobial peptide action and resistance. *Pharmacological reviews*, 55(1): 27–55.

A Appendix

A.1 Sequence Attributes

According to biological studies (Yeaman and Yount 2003; Gidalevitz et al. 2003; Wimley 2010), there are several physical properties crucial for the antimicrobial activity of peptides based on the mechanism. For example, amino acids with positive charges are more likely to bind with bacterial membrane as most bacterial surfaces are anionic, while those with high hydrophobicities tend to move from the solution environment to the bacterial membrane. Here, we introduce three important sequence attributes for AMPs.

Charge The bacterial membrane usually takes the negative charge. Peptides with the positive charge are more likely to bind with the membrane. The whole charge of the peptide sequence S is defined as the sum of the charge of all its residues $C(x_i)$ at pH 7.4, which is

$$C(S) = \sum_{x_i \in S} C(x_i). \quad (7)$$

We only take integer charge into consideration.

Hydrophobicity The hydrophobicity reflects the tendency to bind lipids on the bacterial membrane. A peptide with a high hydrophobicity is easily to move from the solution environment to the bacterial membrane. We use the hydrophobicity scale $H(x_i)$ in Eisenberg, Weiss, and Terwilliger (1984) to calculate the hydrophobicity of a sequence, which is

$$H(S) = \sum_{x_i \in S} H(x_i). \quad (8)$$

Amphipathicity / Hydrophobic Momentum The amphipathicity measures the ability of the peptide to bind water and lipid at the same time, which is a definitive feature of antimicrobial peptides (Hancock and Rozek 2002). It can be quantified by the hydrophobic momentum $uH(S, \theta)$, defined by Eisenberg, Weiss, and Terwilliger (1984). The hydrophobic momentum is determined by the hydrophobicity $H(x_i)$ of each residue x_i , along with the angle θ between residues. The angle can be estimated by the secondary structure. For the α -helix structure, θ is 100° and for β -sheet, θ is 180° .

$$uH(S, \theta) = \sqrt{R_{cos}^2(S, \theta) + R_{sin}^2(S, \theta)}, \quad (9)$$

$$R_{cos}(S, \theta) = \sum_{x_i \in S} H(x_i) * \cos(i * \theta), \quad (10)$$

$$R_{sin}(S, \theta) = \sum_{x_i \in S} H(x_i) * \sin(i * \theta). \quad (11)$$

For each peptide, we calculate the above attributes to measure its antimicrobial activity. For comparison, we draw the distribution on the APD and decoy dataset and select a range for each attribute based on the biological mechanism (Section A.2). We use the percentage of peptides in each attribute range to exploit the generation performance, and use **Combination** to measure the percentage of peptides that satisfy three conditions at the same time.

A.2 Attribute Distribution

To determine the effective threshold of charge, hydrophobicity, and hydrophobic moment of AMP, we analyze the sequence distribution in APD and decoy in Figure 4. For charge, we follow the rule summarized by experts and choose sequences whose net charge is +2 to +10. For the remaining two characters, we draw a histogram and compare the proportion in each box. If the proportion of APD is larger than that in the decoy, we add bin to the acceptance range of the evaluation metric. The final ranges are $C \in [2, 10]$, $H \in [0.25, \infty]$, and $uH \in [0.5, 0.75] \cup [1.75, \infty]$.

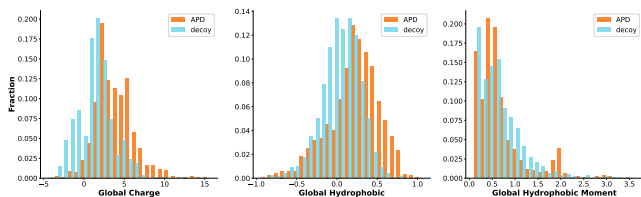


Figure 4: The histogram of charge, hydrophobicity and hydrophobic moment on APD and decoy dataset.

A.3 Secondary Structure Filter

Similar to proteins, the biological functions of AMPs are determined by their amino acid sequences and folded structures (Boman 2003). If the peptide can not fold into an appropriate structure, it is still difficult to take effect. For example, by forming a helical structure, the peptide can gather hydrophobic amino acids on one side and hydrophilic amino

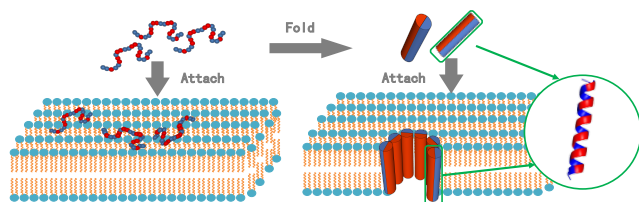


Figure 5: An example of the antimicrobial mechanism. The blue indicates the hydrophobic amino acids, and the red ones are hydrophilic. On the left, although the peptides with reasonable amino acids has attached to the bacterial membrane, they still can not insert into it. However, by folding into the helix structure, as shown on the right, the peptides maintain a stable hole which breaks the membrane of the bacterium.

acids on the other. This amphiphilic structure helps the peptide insert into the membrane and maintain a stable hole with other molecules in the membrane, as shown in Figure 5. Without it, the peptide can hardly penetrate the membrane and attach to the surface.

But does controlling secondary structure also affect sequence attributes? To answer this question, we control the secondary structure of the generated peptides to α -helix for our baseline. The performance gaps are shown in Table 8. From Table 8, we can find that most of the results are improved by limiting sequences to the α -helix structures. It shows that by controlling the structure, the sequence attributes can be improved, which verifies the importance of introducing secondary structures to the controlled generation process. However, the sequence size has decreased significantly, indicating that this generate-then-filter pipeline is inefficient.

A.4 Results of Sequence Attributes

Following the previous AMP design (Das et al. 2018; Van Oort et al. 2021; Capecchi et al. 2021; Das et al. 2021), we use the above three sequence attributes to evaluate the generation performance. As listed in Table 9, LSSAMP outperforms 1.88% on the combination percentage, which indicates that our model can generate sequences satisfying multiple properties at the same time. Besides, the combination percentage is similar to APD, which means that our model learns the sequence distribution of APD. LSSAMP tends to generate peptides with higher hydrophobicity, while AMP-GAN and MLPeptide sample more cationic sequences. Besides, LSSAMP can better capture the amphiphilic secondary structure indicated by the highest uH . Compared with other models, PepCVAE inefficiently generates redundant sequences, which results in a significant decrease in the number of unique sequences. Furthermore, we can find that by further controlling the secondary structure, H, uH and Combination can be improved. This verifies that secondary structure information has a great influence on sequence attributes.

Structure Condition As described above, controlling the secondary structure can affect the attributes of generated peptides. Thus we limit the percentage of the coil structure with different ratio and calculate the sequence attributes of

	Uniq	C	H	uH	Combination
Random $p = 0.1$	2055	7.38% \pm 11.01%	37.93% \pm 0.44%	4.61% \pm 0.31%	4.34% \pm 0.41%
Random $p = 0.2$	1831	6.87% \pm 0.31%	9.52% \pm 0.31%	1.91% \pm 1.06%	2.19% \pm 0.66%
VAE (Dean and Walper 2020)	475	18.45% \pm 2.92%	2.68% \pm 3.28%	-2.78% \pm 1.64%	0.29% \pm 0.74%
AMP-GAN (Van Oort et al. 2021)	1966	2.79% \pm 0.50%	2.16% \pm 0.34%	-2.29% \pm 0.53%	0.17% \pm 0.35%
PepCVAE (Das et al. 2018)	208	3.87% \pm 1.58%	-1.93% \pm 1.61%	1.01% \pm 2.80%	3.93% \pm 1.82%
MLPeptide (Capecchi et al. 2021)	2106	-2.48% \pm 0.39%	2.01% \pm 0.57%	9.24% \pm 1.22%	1.12% \pm 0.38%
LSSAMP	4876	0.30% \pm 0.37%	3.96% \pm 0.64%	7.53% \pm 0.41%	1.87% \pm 0.07%

Table 8: The delta ratio of sequence properties filtered by secondary structures. **Uniq** is the uniq peptide number among 5000 generated sequences. **C**, **H**, **uH** correspond to charge, hydrophobicity, hydrophobic moment. **Combination** is the percentage satisfying three ranges at the same time.

	Uniq	C	H	uH	Combination
APD	3222	68.75%	27.96%	4.72%	6.15%
Decoy	2020	21.83%	8.81%	1.98%	0.10%
Random $p = 0.1$	4978	65.86% \pm 0.19%	26.80% \pm 0.23%	23.10% \pm 0.58%	4.38% \pm 0.16%
Random $p = 0.2$	5000	62.13% \pm 0.39%	24.87% \pm 0.29%	20.79% \pm 0.76%	2.47% \pm 0.17%
VAE	4988	38.00% \pm 0.36%	21.07% \pm 0.58%	12.43% \pm 0.66%	0.34% \pm 0.11%
AMP-GAN	4976	87.66% \pm 0.45%	17.31% \pm 0.74%	23.45% \pm 0.73%	1.92% \pm 0.05%
PepCVAE	1346	15.61% \pm 0.06%	14.54% \pm 0.55%	11.65% \pm 0.23%	2.75% \pm 0.25%
MLPeptide	4486	77.95% \pm 0.72%	8.11% \pm 0.27%	32.91% \pm 0.60%	2.90% \pm 0.16%
LSSAMP	4876	81.88% \pm 0.31%	25.06% \pm 0.45%	37.10% \pm 0.33%	6.26% \pm 0.07%
LSSAMP w/o cond	4903	82.04% \pm 0.42%	21.32% \pm 0.34%	30.51% \pm 0.51%	4.46% \pm 0.20%

Table 9: Physical attributes of generated sequences. We use the percentage of peptides meeting the range to measure the performance. **Uniq** is the number of unique generated sequences. **C**, **H**, **uH** correspond to charge, hydrophobicity, hydrophobic moment described in Section A.1. **Combination** is the percentage satisfying three ranges at the same time. The best results are bold.

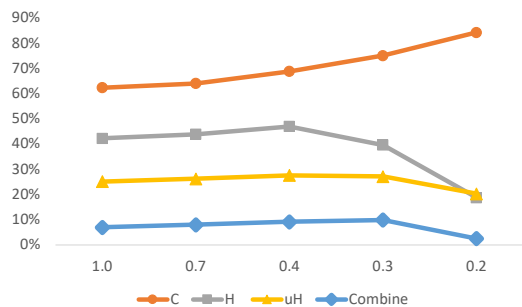


Figure 6: The physical properties of peptides with different percentage of the coil structure. The x-axis is the maximum percentage and y-axis is the percentage of peptides that meet the property range.

generated peptides. The results are shown in Figure 6. We can find that with the decrease of number of coil structures, the percentage of positive peptides keep growing. However, for hydrophobicity and hydrophobic moment, the percentage drop after 0.3. Therefore, we limit the length of the coil structure to 30% in our main experiments.

Visualization of Residue Distribution To illustrate the distribution of residues in the generated peptides, we plot tSNE, shown in Figure 7. We transform the vector with each dimension representing the probability of a certain residue to represent the peptide. Then we use tSNE to convert the high-dimensional vector to 2D and visualize them. We find that there is a large overlap between **LSSAMP w/o condition** and **APD**, which indicates that our model has captured the global distribution of **APD** instead of collapsing to a local mode. Furthermore, **LSSAMP** covers **APD** and has some outliers. The results show that with the secondary structure condition, our model can not only learn the existing **AMP** distribution, but also explore more possible spaces.

Visualization of LSSAMP Distribution We plot the distribution of residues, charge, sequence length, hydrophobicity, and hydrophobic momentum for **APD**, **Decoy**, and our models in Figure 8. Without condition, the distribution of **LSSAMP** is similar to **APD**, which indicates that **LSSAMP** successfully learns sequence distribution of **AMP**. However,

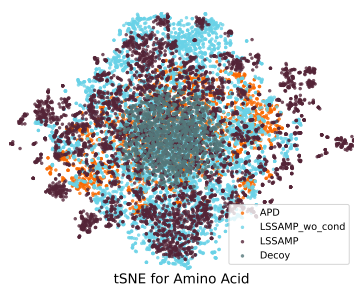


Figure 7: The tSNE plot for the distribution of residue in each sequence on four datasets.

if we control the secondary structure, it is more likely to generate sequences with longer lengths and more positive charges. For hydrophobicity and hydrophobic momentum, the distribution of the generated sequences is more concentrated.

A.5 Wet Laboratory Experiments

We use minimum inhibitory concentration (MIC) to indicate peptide activity, which is defined as the lowest concentration of an antibiotic that prevents the visible growth of bacteria. A lower MIC means a higher antimicrobial activity. To determine MIC, the broth microdilution method was used. A colony of bacteria was grown in LB (Lysogeny broth) medium overnight at 37 degrees. A peptide concentration range of 0.25 to 128 mg/liter was used for MIC assay. The concentration of bacteria was quantified by measuring the absorbance at 600 nm and diluted to $OD_{600} = 0.022$ in MH medium. The sample solutions (150uL) were mixed with a 4uL diluted bacterial suspension and finally inoculated with about $5 * 10^5$ CFU. The Plates were incubated at 37 degrees until satisfactory growth 18h. For each test, two columns of plates were reserved for sterile control (broth only) and growth control (broth with bacterial inoculum, no antibiotics). The MIC was defined as the lowest concentration of the peptide dendrimer that inhibited the growth of bacteria visible after treatment with MTT.

We test the MIC against three common Gram-negative bacteria: *Acinetobacterbaumannii* (*A. Baumannii*), *Pseudomonasaeruginosa* (*P. aeruginosa*) and *E. coli*. We select 21 peptides generated by LSSAMP, and add 3 known AMP sequences and positive control with 3 non-AMP as negative control. The results are shown in Table 4 in the main text, which indicates that 2 out of 21 showed strong antimicrobial activity against bacteria.

A.6 Reproduction

We run the model several times and calculate the mean and variance of the main experimental results and analysis. We also release our code in <https://github.com/dqwang122/LSSAMP>.

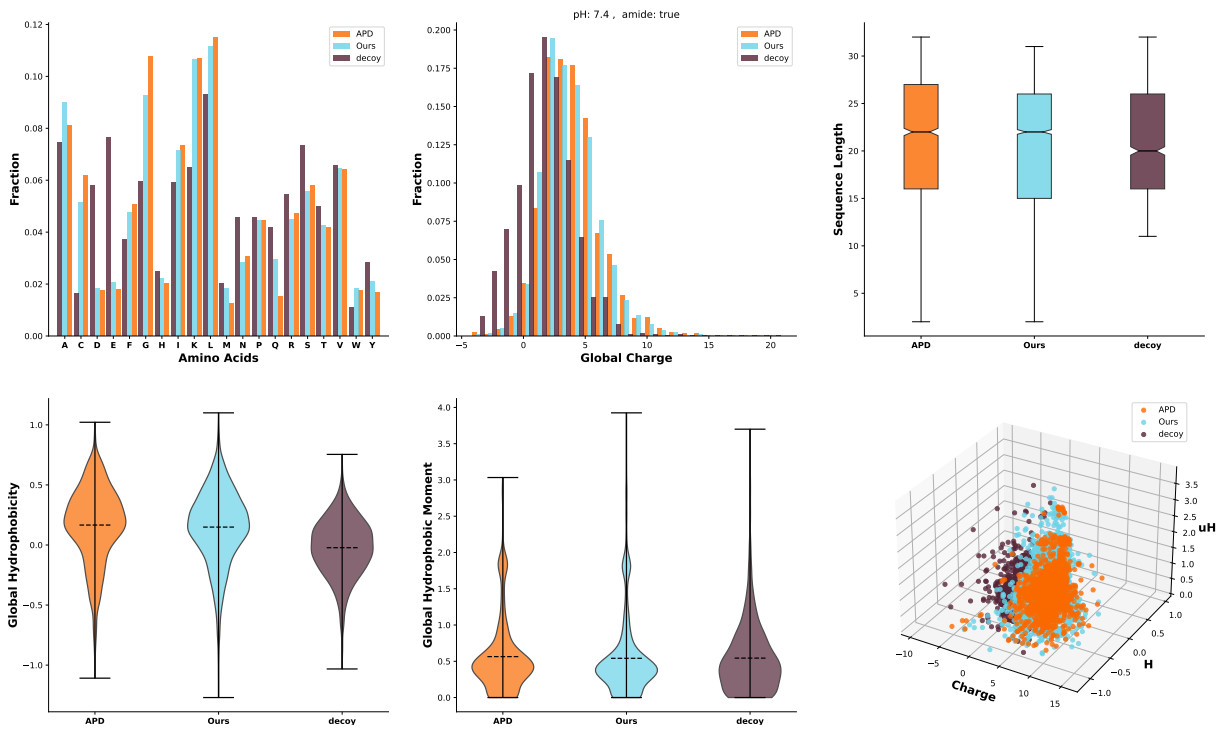


Figure 8: The distribution of residues, charge, sequence length, hydrophobicity, hydrophobic momentum, and a 3D visualization for three sequence attributes.